Supporting Information

Jiang et al. 10.1073/pnas.0909310107

SI Results

cAMP TR-FRET Assay Optimization. We began by creating 13 independent C6 glioma (C6G) cell lines that stably express recombinant human EP2 receptors. Following transfection, isolates were purified by limiting dilution in selection medium containing 1 mg/mL G418, then expanded for testing. A single line was selected for further characterization based on growth characteristics, large response to a saturating concentration of prostaglandin E2 (PGE_2), and preservation of the EP2 response in acutely dissociated cells. A second stable line of human colon tumor (HCT-15) cells that expresses human EP2 was developed similarly to ensure that results were not dependent on cell type.

EP2 activation stimulates adenylate cyclase activity, resulting in elevated cAMP levels. We used a TR-FRET (time-resolved fluorescence resonance energy transfer) method developed by CisBio to monitor PGE_2-induced cAMP accumulation in C6G cells expressing human EP2 receptors. The assay is based on generation of a strong FRET signal upon the interaction of two molecules: a cAMP antibody coupled to a FRET donor, and a cAMP analog coupled to a FRET acceptor. Endogenous cAMP competes with labeled cAMP for binding to the cAMP antibody, and thus reduces the FRET signal. Incubation of the C6G-EP2 cells with the selective EP2 receptor agonist, butaprost, resulted in a time- and concentration-dependent reduction in FRET signal (Fig. S1*A*). Equilibrium conditions were reached at room temperature within 30 to 40 min, so 40-min incubation was selected for subsequent experiments. The plateau response magnitude was concentration-dependent, consistent with incomplete block of phosphodiesterase activity in the reaction despite the presence of 20-μM rolipram. For this reason we measured the plateau FRET level rather than the time constant of approach to plateau. The endogenous agonist, PGE_2, was approximately 8-fold more potent than butaprost (Fig. S1*B*), and was used in screening in the event allosteric potentiators of EP2 proved to be agonist-dependent.

Two measures of assay robustness, the Z' factor (1) and signal-to-noise ratio (S:N), were used to optimize the assay for screening, initially in 384-well plates then in 1,536-well format. In either format, these assay robustness measures were adequate for high-throughput screening (Z' > 0.5, S:N > 8) at a suspension cell density of 3,000 to 9,000 cells per well (Fig. S1*C*). Both Z' and S:N were stable over a 3-month optimization period, during which 10 experiments were conducted with cells of increasing passage number. Fig. S1*D* demonstrates that the quality of the assay remained high over the entire primary screen of 239 high-density (1,536-well) plates.

Unconventional Agonist-Like Allosteric Effect of the Thiophene Carboxylates. In C6G-EP2 cells, all of the allosteric potentiators increased cAMP level by themselves to a variable degree in the absence of added PGE_2. Fig. 2*C* shows an example of a relatively small "basal effect" of the potentiators, but the effect could occasionally be as large as a 70% reduction in the TR-FRET signal. For example, in the absence of added PGE_2, 20-μM compound **1** reduced the TR-FRET signal to 55 ± 4.7% of control ($n = 13$) in C6G-EP2 cells, and compound **2** reduced the TR-FRET signal to 73 ± 3.8% of control ($n = 9$) (Fig. S6). The EP2 potentiators had no effect on parent C6G cells or C6G cells expressing β2-adrenergic rather than EP2 receptors (Fig. 1 *B* and *C*), ruling out an action on a Gαs-coupled receptor other than EP2. We then carried out a number of experiments to determine whether the basal effect of these compounds represents a conventional direct agonist effect on EP2, or was instead another manifestation of allosteric potentiation.

Several lines of evidence indicate that these compounds are not conventional agonists binding within the PGE_2 binding site. First, elevation of cAMP by the potentiators did not occur or was minimal in an independently created cell line, HCT-15-EP2. For comparison with the C6G-EP2 cells, the TR-FRET signal in 20-μM compound **1** was 94 ± 2.8% of control in HCT-15-EP2 cells ($n = 11$), and in 20-μM compound **2** was 95 ± 2.5% of control ($n = 16$) (Fig. S6). This is unexpected if the potentiators act directly as an agonist. PGE_2 and butaprost displayed similar potencies in both EP2 cell lines, which argues against a substantially lower receptor density or less efficient coupling in the HCT-15 cell line that might have obscured a direct agonist effect. Second, the thiophene carboxylate structure does not resemble the prostaglandin backbone, and potentiators with a variety of dissimilar structures were identified in the primary and secondary screening phase; all raised cAMP in the absence of added PGE_2. Neither result of course is definitive. Third, C6G is a rat glial cell line that produces prostaglandins, especially PGE_2 (2). Fifty thousand cells constitutively secrete enough PGE_2 into the medium over a 24-h period to result in a standing PGE_2 concentration of 1.1 nM (3). Therefore, the basal effect of the allosteric EP2 compounds could be because of potentiation of the effect of endogenous PGE_2. Indeed, we could mimic the basal effect in HCT-15-EP2 cells by pretreatment with PGE_2 (0.3–3 nM). Fig. S7*A* shows the typical potentiation profile of compound **1** in untreated HCT-15-EP2 cells. By contrast, pretreatment of the cells with 1 nM PGE_2 for 20 min before addition of compound **1** caused a substantial basal effect, undoubtedly because of potentiation of the effect of added PGE_2 (Fig. S7*B*). Moreover, butaprost, a selective EP2 agonist, elevates cAMP level but does not shift the PGE_2 concentration-response curve to the left (Fig. S7*C*). Indeed, just the opposite effect was observed, in that 15-nM butaprost shifted the PGE_2 concentration-response curve to the right by 1.43- ± 0.087-fold ($n = 6$). These observations taken together make it highly unlikely that the observed leftward shift of the PGE_2 concentration-response curve in the presence of the thiophene carboxylates is caused by a direct agonist effect at the conventional orthosteric binding site.

Finally, we considered then rejected a series of less likely explanations for the basal effect of the EP2 allosteric potentiators. Recognizing that C6G cells produce high levels of endocannabinoids (4), and that the endocannabinoid structure is similar to that of prostaglandins, we tested the hypothesis that the EP2 potentiators also inhibited fatty acid amide hydrolase, thereby allowing buildup of an endocannabinoid that might act as an agonist at CB1 and EP2 receptors. However, the CB1 antagonist AM251 (2 μM) did not alter the basal effect of compound **1** (Fig. S7*D*). C6G also express adenosine, VIP together with their Gαs-coupled receptors; however, pretreatment of C6G-EP2 cells with antagonists of these receptors did not reduce the basal effect of compound **1** (Fig. S7*D*). Thus the basal effect of the EP2 potentiators does not involve amplification of the actions of other known Gαs-coupled mediator-receptor systems that are expressed by C6G cells.

Although C6G cells have the ability to synthesize PGE_2, the measured PGE_2 level under our assay conditions (acute dissociation with EDTA followed by 2-h incubation at room temperature) was near background in C6G-EP2 cells. Thus, it is unsurprising that a mixture of inhibitors of COX1 and COX2 (each present at a concentration 20× their K_d) did not prevent the basal effect of compound **1** (Fig. S7*D*). Taken together, these data demonstrate that the basal effect of the allosteric potentiators on

C6G-EP2 cells involves potentiation of the activation of EP2 receptors, probably by a molecule not derived from COX1 or COX2. The identity of this endogenous EP2 agonist is unknown but is unlikely to be an endocannabinoid.

Cell Viability. Our results show that these allosteric compounds are highly EP2 selective and neuroprotective from excitotoxicity. However, it is necessary to investigate the possible cytotoxicity of these EP2 allosteric compounds to evaluate in vitro safety before animal testing. Cellular toxicity of the EP2 allosteric potentiators was assessed in C6G cells with the CellTiter-Glo luminescent cell viability assay and Alamar blue assay. The CellTiter-Glo assay measures the cellular ATP level, an indicator of cell viability, whereas the Alamar blue assay measures the reducing ability of live cells. C6G cells were incubated with EP2 allosteric potentiators or positive control doxorubicin for 48 h before the measurement. The IC_{50}s of most tested allosteric potentiators were over 100-μM bulk concentration (Table 2). Significantly, the IC_{50}s for cellular toxicity of two prominent allosteric EP2 potentiators, compounds **1** and **3**, were 248 μM and 4,420 μM, respectively (Fig. 2*B* and Table 2). The positive control doxorubicin showed significant toxicity with the expected low IC_{50} (0.35 μM) (Table 2).

SI Materials and Methods

Cell Lines. The rat C6G cell line and the human colon tumor (HCT-15) cell line were purchased from American Type Culture Collection. The C6G cell line stably expressing β2-adrenergic receptor (C6β2-AR) was a kind gift from K. Minneman from Emory University. The human embryonic kidney (HEK) cell line stably expressing the human EP4 receptor (HEK-EP4) was a kind gift from Merck & Co., Inc.

Cell Culture and Transfection. Both C6G cells and HEK cells were grown in Dulbecco's Modified Eagle Medium (Invitrogen), supplemented with 10% (vol/vol) FBS (FBS) (Invitrogen), 100 U/mL penicillin, and 100 μg/mL streptomycin (Invitrogen). C6β2-AR cells and HEK-EP4 cells were maintained in complete DMEM medium containing 250 μg/mL G418 and 200 μg/mL hygromycin (Invitrogen). HCT-15 cells were grown in RPMI medium 1640 (Sigma-Aldrich), supplemented with 20% (vol/vol) FBS, 1 mM sodium pyruvate, 23.81 mM sodium bicarbonate, 10 mM hepes, 100 U/mL penicillin, and 100 μg/mL streptomycin. Cells were transfected with EP2 plasmid in the pcDNA3.1 vector using the Lipofectamine 2000 transfection reagent (Invitrogen), and subcloned by limiting dilution. C6G-EP2 and HCT-15-EP2 subclones were expanded and maintained in complete medium supplemented with 1 mg/mL G418.

Chemicals and Drugs. PGE_2, butaprost, rolipram, doxorubicin, forskolin, COX1/2 inhibitors (NS-398, CAY10416, Nimesulide, SC-560, CAY10404), CB1 agonists (anandamide, 2-Arachidonoyl glycerol), and CB1 antagonist AM251 were purchased from Cayman Chemical. Adenosine A2A receptor antagonists (CGS15943, SCH 58261, ZM241385), VIP antagonist [D-p-Cl-Phe6, Leu17], [Ac-Tyr1, D-Phe2] GRF 1–29 amide, and staurosporine aglycone (K252c) were purchased from Tocris. PACAP antagonist PACAP 6–38 was purchase from American Peptide. IBMX, isoproterenol, BSA, Congo Red, and tetraiodophenolphthalein were purchase from Sigma-Aldrich.

Ultra-High-Throughput Screening in 1,536-Well Format. C6G-EP2 cells were dissociated using EDTA and suspended in HBSS. To optimize cell density for ultra high-throughput screening and minimize day-to-day variation, a dose-response curve for PGE_2 was obtained at several cell densities every day before screening. The cell density (generally 2,000–3,000 cells per well) yielding an EC_{50} for PGE_2 of 2 to 3 nM was selected for ultra high-throughput screening. Assay plates were prepared by dispensing 4 μL per well of the cells suspended in HBSS containing 20-μM rolipram into 1,536-well black plates (Corning) using a Multidrop Combi dispenser (Thermo-Fisher Scientific). Next, 0.1 μL of 1 mM library compounds diluted in DMSO or vehicle were transferred to the cell assay plate using a Pintool (V&P Scientific) integrated with Beckman NX liquid handler (Beckman Coulter) and incubated for 5 to 30 min. Then, 1 μL of PGE_2 (final 0.3 nM, an EC_{15}) was dispensed to the wells with library compounds or vehicle as control. PGE_2 at 1 μM final was added to the wells with vehicle as controls for 100% cAMP induction. The final concentration of the library compound was 20 μM. Each 1,536-well plate had a set of controls contained within one 32-well column of the assay plate. After incubating with PGE_2 for 30 min, the d2-labeled cAMP (1 μL) and Cryptate-labeled anti-cAMP (2 μL) diluted in lysis buffer were dispensed sequentially to the assay plates and incubation continued at room temperature for 0.5 to 2 h before TR-FRET measurement. The TR-FRET signal was measured using an Envision 2103 Multilabel plate reader (PerkinElmer Life Sciences) with a laser excitation at 337 nm and dual emissions at 665 nm and 590 nm for d2 and Cryptate, respectively. The FRET signal is expressed as: $F665/F590 \times 10^4$. The effect of each compound on PGE_2-induced cAMP production was expressed as percent inhibition of the TR-FRET ratio scaled between values measured after incubation with vehicle and 1 μM PGE_2 and calculated based on per plate control wells as the following equations:

$$\%\,inhibition\ compound = 100 - (\text{FRET signal compound} - \text{FRET background})/(\text{FRET vehicle} - \text{FRET background}).$$

$$\%\,inhibition\ at\ 1\,\mu M\ PGE_2 = 100 - (\text{FRET signal at } 1\,\mu\text{M } PGE_2 - \text{FRET background})/(\text{FRET vehicle} - \text{FRET background}) \times 100.$$

The FRET background is the average FRET signal from 32 wells with anti-cAMP-Cryptate only, without d2-labeled cAMP. The FRET compound and vehicle are the FRET signals from compound well and the average FRET signal from 32 wells with vehicle control and 0.3 nM of PGE_2, respectively. The FRET signal at 1 μM PGE_2 is the average FRET signal from 32 wells with vehicle and 1 μM PGE_2. All data were deposited into PubChem (http://pubchem.ncbi.nlm.nih.gov/; assay ID numbers: 940, 1080, 1421, and 1422).

Compound Solubility by Nephelometry. Compounds were dissolved in DMSO at a starting stock concentration of 30 mg/mL, and then were serially diluted in DMSO for a concentration profile of 30, 20, 15, 10, 7.5, 5, 2.5, 1.25, 0.63, 0.31, and 0.15 mg/mL. The solutions were transferred to a 96-well microplate and further diluted 100× in PBS at pH 7.4, with the final DMSO concentration 1%. The plates were incubated for 90 min and then analyzed by a BMG LABTECH NEPHELOstar microplate nephelometer. Each concentration was assayed in a replicate of seven wells.

Dynamic Light Scattering. Compound stocks (10 mM in DMSO) were diluted to 20 μM in filtered HBSS buffer. Samples were analyzed with a 4 mW helium-neon (He-Ne) laser at 633 nm with a ZEN 3690 from Malvern Instruments at 25 °C, using a detector angle of 90°. The laser attenuation was 11 (no blockage) and the measurement duration was 50 s. Particle size was interpreted and calculated with Dispersion Technology Software 4.20 included by the manufacturer. Each diameter and intensity value represents four independent measurements.

Transmission Electron Microscopy. Compounds (10 mM in DMSO) were diluted to 20 μM in HBSS at room temperature. Five microliters of each was applied to a carbon-coated grid and negatively stained with 1% phosphotungstic acid. Images were obtained with a Hitachi H-7500 transmission electron microscope (120 kV) (Hitachi High-Tech).

Determination of Compound Monomer Percent. Compound stocks (10 mM in DMSO) were diluted to 20 μM in filtered HBSS buffer. Half of the solution was centrifuged at 100,000 × *g* for 10 min. After ultracentrifugation, the supernatant was collected and was shown to be devoid of detectable nanoparticles. Twenty microliters of uncentrifuged solution and the same amount of supernatant were analyzed by Agilent LC-MS. The absorbance was measured at 254.4 nm and the ratio of the amount of compound in supernatant and the amount in uncentrifuged solution was used to calculate the monomer percentage in the diluted compound solution.

Cell-Based Label-Free Assay. As a complementary method to the TR-FRET cAMP assay, the effects of EP2 compounds on PGE_2 dose–response in C6G-EP2 and HCT-15-EP2 cells were also measured by a label-free optical biosensor technology (Corning). Cells (40 μL per well) were seeded into Corning Epic 384-well fibronectin-coated biosensor cell assay microplates with 8,000 cells per well in appropriate medium and grown overnight. The cells were washed gently twice with 50 μL per well of assay buffer (HBSS with 20-mM HEPES), then 30-μL assay buffer was dispensed into the wells using the Multidrop Combi. The plate was loaded into the Epic reader and thermo-equilibrated for 1 h, then baseline readings were obtained (10 min, 10 data points). EP2 test compounds (10 μl) diluted in assay buffer were added by 384-channel array of Sciclone liquid handler (Caliper Life Sciences) and incubations continued for 30 min, then 10 μL of assay buffer or PGE_2 in different concentrations was added using Sciclone. The plate was immediately reloaded into the Epic reader and measurements continued for 50 to 70 min. The Epic data were recorded kinetically every minute and reported as picometer (pm) units. Maximum DMR signal (Δresponse) expressed as Δpm was calculated by the subtracting the recorded picometer before PGE_2 addition from recorded picometer after 40 min PGE_2 addition.

PGE_2 Measurement. The PGE_2 level produced by C6G-EP2 cells was measured by PGE_2 ELISA (Cayman Chemicals). C6G-EP2 cells were cultured overnight in a T-75 flask in complete media. The next day the cells were dissociated with EDTA and plated in a T-25 flask (at a density of 2×10^6 cells/T-25) in HBSS, then incubated at 37 °C for 3 h. The entire contents of the flasks was collected and centrifuged. The supernatant was assayed by ELISA according to the manufacturer's protocol. Luminescence intensity was measured by a microplate reader (Molecular Devices) with an integration time of 1 s. A standard curve for PGE_2 was run with each experiment.

Cell Viability Assays. The cellular toxicity of EP2 compounds was examined with the CellTiter-Glo assay kit (Promega), which uses the luciferase reaction to measure cellular ATP level. We also used the reduction of nonfluorescent resazurin to resorufin by actively metabolizing cells (Alamar Blue assay, Invitrogen). Both ATP level and reducing ability correlate with cell viability. Both assays gave similar results and the IC_{50}s of the compounds for cell toxicity were calculated. Briefly, untransfected C6G cells were plated in 384-well plates at 2,000 cells per well in 25 μL DMEM media plus EP2 compounds, and incubated for 48 h. CellTiter-Glo reagent (25 μL) was then added to each well. The contents were mixed for 2 min on an orbital shaker to induce cell lysis and incubated at room temperature for 10 min. Relative viability is proportional to luminescence intensity as measured by microplate reader (Molecular Devices) with an integration time of 1 s. The Alamar blue viability assay was carried out in 384-well plates. Forty-five microliter medium containing 1,000 cells was dispensed to 384-well plates and incubated overnight. Next, 0.5 μL of compounds in DMSO with increasing concentrations were added to the cells and incubated for 48 h. CellTiter-Blue (5 μL) (Promega) was dispensed to each well and incubated for 15 h. The fluorescence intensity was then detected using Envision 2103 Multilabel plate reader with excitation at 545 nm and emission at 610 nm. Data were normalized to the vehicle (DMSO) control wells without testing compound.

Immunocytochemistry. Hippocampal neurons were isolated from E16 to 18 embryos of timed-pregnant Sprague-Dawley rats. Cells were plated onto poly-D-lysine coated 24-well plates at a density of 150,000 cells per well in Neurobasal medium plus B27 and 5% FBS (FBS) (Invitrogen). Cultures were incubated at 37 °C in 95% air/5% CO_2, and half of the culture medium was changed every 3 to 4 days. After 14 days in culture, cells were fixed with 4% paraformaldehyde in PBS, followed by permeation with 0.2% Triton X-100. After incubation in blocking buffer (USB) for 3 h, the cells were incubated with EP2 polyclonal antibody (Cayman Chemical) overnight and followed by staining with Alexa Fluor GAR 488 secondary antibody (Invitrogen). Images were obtained with a fluorescent microscope (Carl Zeiss).

Chemical Design and Synthesis. All EP2 compounds were either synthesized in the Emory Chemical Biology Discovery Center or obtained through commercial sources. Synthetic compounds were analyzed by NMR, high-resolution mass spectrometry and elemental analysis. Agilent LC-MS was used to demonstrate that compounds did not degrade throughout the study. Thiophene carboxylates were synthesized straightforwardly as shown in Fig. S2. Cyanomethylesters or cyanomethyl ketones as starting material were prepared from cyanoacetic acid, then treated with cycloalkylketone and sulfur with triethyl amine in methanol to yield 2-aminothiophenes in moderate to good yields. These amines were coupled to a variety of alkyl- and aroylchlorides to yield thioacetamide derivatives. Ninety-four thioacetamide derivatives were synthesized for the structure-activity relationship study. Representative members are shown in Fig. S3 and a set of analogs that provided critical structure-activity information is presented in Table 2. Characterization data (^1H, ^{13}C NMR) for the compounds are described in *Analytical Chemistry*.

Analytical Chemistry. Mass spectrometric analysis was provided by the Emory University Mass Spectrometry Center. Routine proton and carbon NMR spectra measured during synthesis were obtained on a Varian Inova-400 (400 MHz). Solvent for NMR was deuteriochloroform ($CDCl_3$) (residual shifts: δ 7.26 for ^1H and δ 77.7 for ^{13}C). The residual shifts were taken as internal references and reported in parts per million (ppm). TLC and preparative TLC (PTLC) were performed on precoated, glass-backed plates (silica gel 60 F_{254}; 0.25 mm thickness) from EM Science and were visualized by UV lamp. Column chromatography was performed with silica gel (230–400 mesh ASTM) using the "flash" method. Elemental analyses were performed by Atlantic Microlab Inc. All solvents and other reagents were purchased from Aldrich Chemical Co. The reagents were used as received. All reactions were performed under anhydrous nitrogen atmosphere in oven-dried glassware (d, doublet; dd, double-doublet; m, multiplet; q, quartet; s, singlet; t, triplet).

Compound **1**: ^1H NMR (400 MHz, $CDCl_3$) δ 11.93 (s, 1H), 7.54 (m, 1H), 7.22 (dd, J = 3.6, 0.4 Hz,), 6.52 (dd, J = 3.6, 1.6 Hz, 1H), 4.37 (q, J = 7.6 Hz, 2H), 3.0 (m, 2H), 2.69 (m, 2H), 1.81 (m, 2H), 1.61 (m, 4H), 1.38 (t, J = 7.2 Hz, 3H). Anal.

Calcd for $C_{17}H_{19}NO_4S$: C, 61.24; H, 5.74; N, 4.20. Found: C, 61.28; H, 5.65; N, 4.20.

Compound **2**: ^{1}H NMR (400 MHz, $CDCl_3$) δ1.55-1.70 (m, 13H), 1.82-1.87 (m, 2H), 2.74 (t, J = 5.6 Hz, 2H), 3.05 (t, J = 5.6 Hz. 2H), 6.56 (dd, J = 2.0, 3.6 Hz, 1H), 7.26 (m, 1H), 7.59 (dd, J = 0.8, 1.6 Hz, 1H), 11.86 (s, 1H). Anal. Calcd for $C_{19}H_{23}NO_4S$: C, 63.13; H, 6.41; N, 3.88. Found: C, 62.54; H, 6.31; N, 3.87.

Compound **3**: ^{1}H NMR (400 MHz, $CDCl_3$) δ 12.06 (s, 1H), 7.55 (m, 1H), 7.23 (dd, J = 3.2, 0.8 Hz, 1H), 6.52 (dd, J = 3.6, 1.6 Hz, 1H), 3.85 (s, 3H), 2.73 (m, 2H), 2.62 (m, 2H), 1.75 (m, 4H). Anal. Calcd for $C_{15}H_{15}NO_4S$: C, 59.00; H, 4.95; N, 4.59. Found: C, 59.04; H, 4.93; N, 4.48.

Compound **4**: ^{1}H NMR (400 MHz, $CDCl_3$) δ 12.19 (s, 1H), 7.96 (m, 2H), 7.13 (m, 2H), 4.35 (q, J = 7.2 Hz, 2H), 3.02 (m, 2H), 2.70 (m, 2H), 1.80 (m, 2H), 1.63 (m, 4H), 3.76 (t, J = 7.2 Hz, 3H). Anal. Calcd for $C_{19}H_{20}FNO_3S$: C, 63.14; H, 5.58; N, 3.88. Found: C, 63.03; H, 5.46; N, 3.78.

Compound **5**: ^{1}H NMR (400 MHz, $CDCl_3$) δ 11.88 (s, 1H), 7.54 (m, 1H), 7.28 (dd, J = 1.4, 0.4 Hz, 1H), 6.56 (dd, J = 3.6, 1.6 Hz, 1H), 3.12 (m, 2H), 2.74 (m, 2H), 1.80 (m, 2H), 1.66 (m, 4H). HRMS Cacld for $C_{15}H_{16}NO_5S$ (M+H) 306.07946. Found 306.07951

Compound **6**: ^{1}H NMR (400 MHz, $CDCl_3$) δ 12.72 (s, 1H), 7.57 (m, 1H), 7.22 (dd, J = 3.6, 0.8 Hz, 1H), 6.51 (dd, J = 3.6, 1.6 Hz, 1H), 2.88 (m, 2H), 2.76 (m, 2H), 2.71 (m, 2H), 1.82 (m, 2H), 1.72 (m, 2H), 1.66 (m, 4H), 0.95 (t, J = 7.6 Hz, 3H). Anal. Calcd for $C_{18}H_{21}NO_3S$: C, 65.23; H, 6.39; N, 4.23. Found: C, 64.61; H, 6.29; N, 4.20.

Compound **7**: ^{1}H NMR (400 MHz, $CDCl_3$) δ 11.99 (s, 1H), 7.55 (dd, J = 1.4, 0.4 Hz, 1H), 7.24 (dd, J = 1.4, 0.4 Hz, 1H), 6.53 (dd, J = 3.6, 1.6 Hz, 1H), 5.0 (m, 1H), 3.07 (m, 2H), 2.72 (m, 2H), 1.95-1.44 (m, 16H). Anal. Calcd for $C_{21}H_{25}NO_4S$: C, 65.09; H, 6.50; N, 3.61. Found: C, 64.81; H, 6.52; N, 3.61.

Compound **8**: ^{1}H NMR (400 MHz, $CDCl_3$) δ1.80-1.83 (m, 4H), 2.66-2.68 (m, 2H), 2.82-2.86 (m, 2H), 6.57 (dd, J = 2.0, 3.6 Hz, 1H), 7.28 (d, J = 3.6 Hz, 1H), 7.58 (m, 1H), 11.97 (s, 1H). Anal. Calcd for $C_{14}H_{13}NO_4S$: C, 57.72; H, 4.50; N, 4.81. Found: C, 58.78; H, 4.76; N, 4.65.

Compound **9**: ^{1}H NMR (400 MHz, $CDCl_3$) δ1.24-1.29 (m, 2H), 1.43-1.48 (m, 2H), 1.61-1.65 (m, 13H), 2.74 (t, J = 6 Hz, 2H), 2.90 (t, J = 6.4 Hz, 2H), 6.54 (dd, J = 1.6, 3.2 Hz, 1H), 7.26 (m, 1H), 7.59 (m, 1H), 12.19 (s, 1H). Anal. Calcd for $C_{20}H_{25}NO_4S$: C, 63.97; H, 6.71; N, 3.73. Found: C, 63.94; H, 6.76; N, 3.79.

Compound **10**: ^{1}H NMR (400 MHz, $CDCl_3$) δ 12.09 (s, 1H), 7.55 (m, 1H), 7.23 (d, J = 3.6 Hz, 1H), 6.51 (dd, J = 3.6, 1.6 Hz, 1H), 3.87 (s, 3H), 2.86 (m, 2H), 2.70 (m, 2H), 1.57 (m, 4H), 1.43 (m, 2H), 1.21 (m, 2H). Anal. Calcd for $C_{17}H_{19}NO_4S$: C, 61.24; H, 5.74; N, 4.20. Found: C, 61.32; H, 5.80; N, 4.21.

Compound **11**: ^{1}H NMR (400 MHz, $CDCl_3$) δ 11.96 (s, 1H), 7.53 (m, 1H), 7.21 (dd, J = 1.4, 0.4 Hz, 1H), 6.50 (dd, J = 3.6, 1.6 Hz, 1H), 3.86 (s, 3H), 2.98 (m, 2H), 2.68 (m, 2H), 1.80 (m, 2H), 1.60 (m, 4H). Anal. Calcd for $C_{16}H_{17}NO_4S$: C, 60.17; H, 5.37; N, 4.39. Found: C, 60.41; H, 5.32; N, 4.23.

Compound **12**: ^{1}H NMR (400 MHz, $CDCl_3$) δ 12.0 (s, 1H), 7.07 (dd, J = 3.8, 0.8 Hz, 1H), 7.55 (dd, J = 4.8, 1.2 Hz, 1H), 7.10 (dd, J = 4.8, 3.6 Hz, 1H), 3.85 (s, 3H), 2.71 (m, 2H), 2.61 (m, 2H), 1.75 (m, 4H). Anal. Calcd for $C_{15}H_{15}NO_3S_2$: C, 56.05; H, 4.70; N, 4.36. Found: C, 56.10; H, 4.69; N, 4.24.

Compound **13**: ^{1}H NMR (400 MHz, $CDCl_3$) δ 12.24 (s, 1H), 7.97 (m, 2H), 7.48 (m, 3H), 3.83 (s, 3H), 2.72 (m, 2H), 2.62 (m, 2H), 1.74 (m, 4H). Anal. Calcd for $C_{17}H_{17}NO_3S$: C, 64.74; H, 5.43; N, 4.44. Found: C, 64.66; H, 5.39; N, 4.47.

Statistical Analysis. All data from cell-based assays were plotted with Origin software. Statistical analysis of the LDH assay was performed using GraphPad Prizm software with one-way ANOVA and posthoc Bonferroni. $P < 0.01$ was considered to be statistically significant. All data are presented as mean ± SEM.

1. Zhang JH, Chung TD, Oldenburg KR (1999) A Simple statistical parameter for use in evaluation and validation of high throughput screening assays. *J Biomol Screen* 4:67–73.
2. Liu Y, Tonna-DeMasi M, Park E, Schuller-Levis G, Quinn MR (1998) Taurine chloramine inhibits production of nitric oxide and prostaglandin E2 in activated C6 glioma cells by suppressing inducible nitric oxide synthase and cyclooxygenase-2 expression. *Brain Res Mol Brain Res* 59:189–195.
3. Badie B, et al. (2003) Microglia cyclooxygenase-2 activity in experimental gliomas: possible role in cerebral edema formation. *Clin Cancer Res* 9: 872–877.
4. Jacobsson SO, Wallin T, Fowler CJ (2001) Inhibition of rat C6 glioma cell proliferation by endogenous and synthetic cannabinoids. Relative involvement of cannabinoid and vanilloid receptors. *J Pharmacol Exp Ther* 299:951–959.

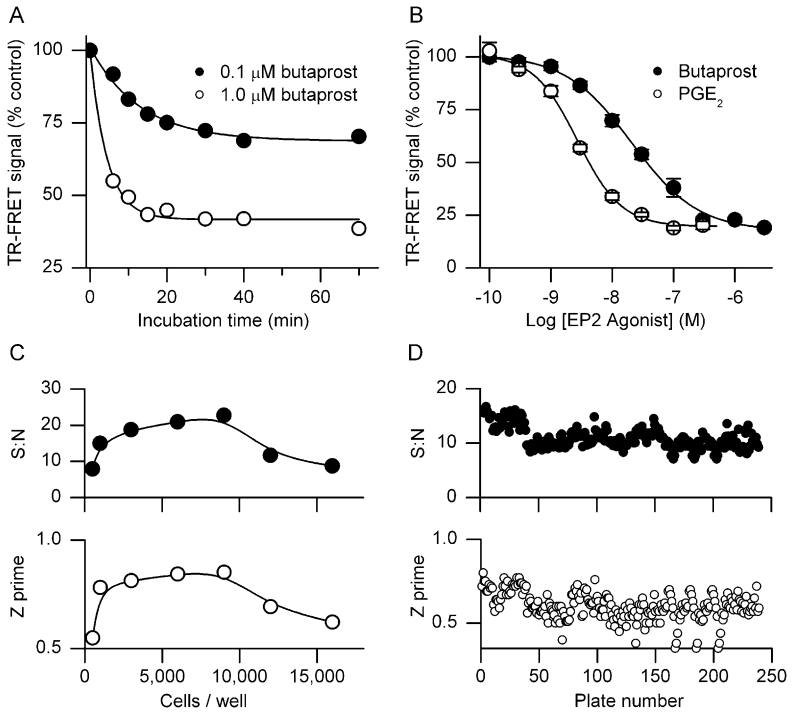

Fig. S1. Optimization of the TR-FRET assay for EP2 receptor activation. (*A*) Butaprost produces a time- and concentration-dependent reduction in TR-FRET signal. Solid circles, $\tau = 13$ min; open circles $\tau = 4.4$ min. (*B*) PGE_2 ($EC_{50} = 2.7$ nM) is a more potent agonist than butaprost ($EC_{50} = 21$ nM). (*C*) Assay robustness parameters are optimal at 3,000 to 9,000 cells per well. (*D*) Z′ and S:N remain adequate over the whole primary screen in 1,536 well plates.

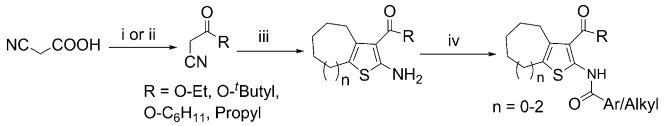

Fig. S2. Synthesis of thioacetamides for structure-activity relationship study. Reagents and conditions: *i*. 2eq. n-BuLi, buteroyl chloride; *ii*. cyclohexanol or t-butanol or ethanol, EDCI, DCM. 80%; *iii*. cyclohexanone/heptanone, Sulfur, Et_3N, MeOH, 60–80%; *iv*. Acylchlorides or ArCOCl, DMAP, DCM, RT, >90%.

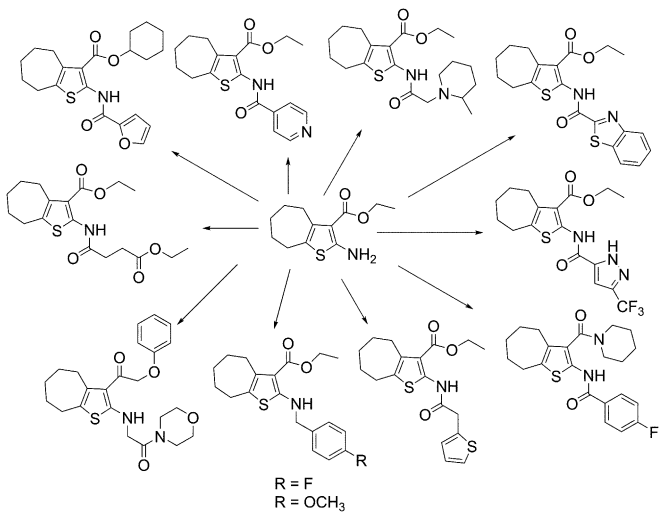

Fig. S3. Representative members of thioacetamides.

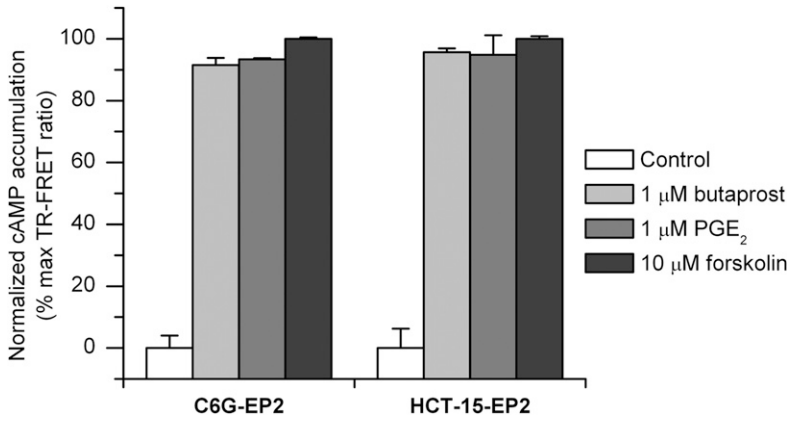

Fig. S4. Accumulation of cAMP in C6G-EP2 and HCT-15-EP2 cells by EP2 activation. Intracellular cAMP levels are increased by treatment with butaprost, PGE_2, and forskolin, an activator of adenylyl cyclase, in both C6G-EP2 and HCT-15-EP2 cell lines. The maximum response of PGE_2 (1 μM) for activating EP2 receptors in both cells is similar to that of 10-μM forskolin.

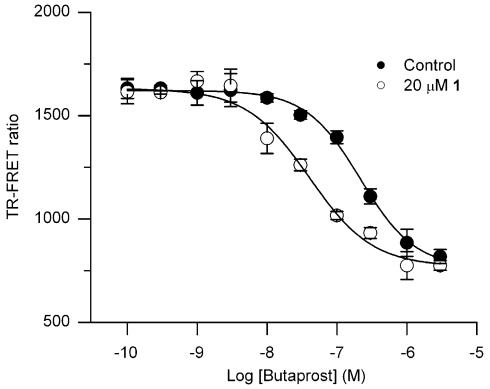

Fig. S5. Effect of EP2 allosteric potentiator on potency of butaprost. Compared to control, 20 μM compounds **1** increased the potency of butaprost on EP2 receptors 4 to 5-fold in HCT-15-EP2 cells. Shown are the mean ± SEM of quadruplicate measurements in a single experiment; the experiment was repeated three times with similar results.

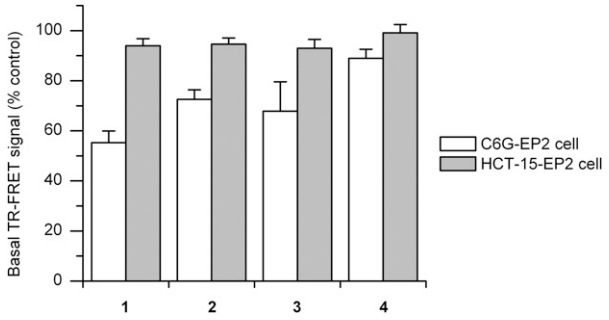

Fig. S6. The effects of EP2 allosteric potentiators on basal cAMP level. Compared to control, 20-μM compounds **1** to **4** increased the cellular cAMP level, indicated by reduced TR-FRET signal, in absence of exogenous PGE_2 in C6G-EP2 cells, whereas there is no such significant increase caused by these EP2 potentiators in HCT-15-EP2 cell line. Bars represent the mean ± SEM. n = 7 to 16 independent experiments, each done in quadruplicate.

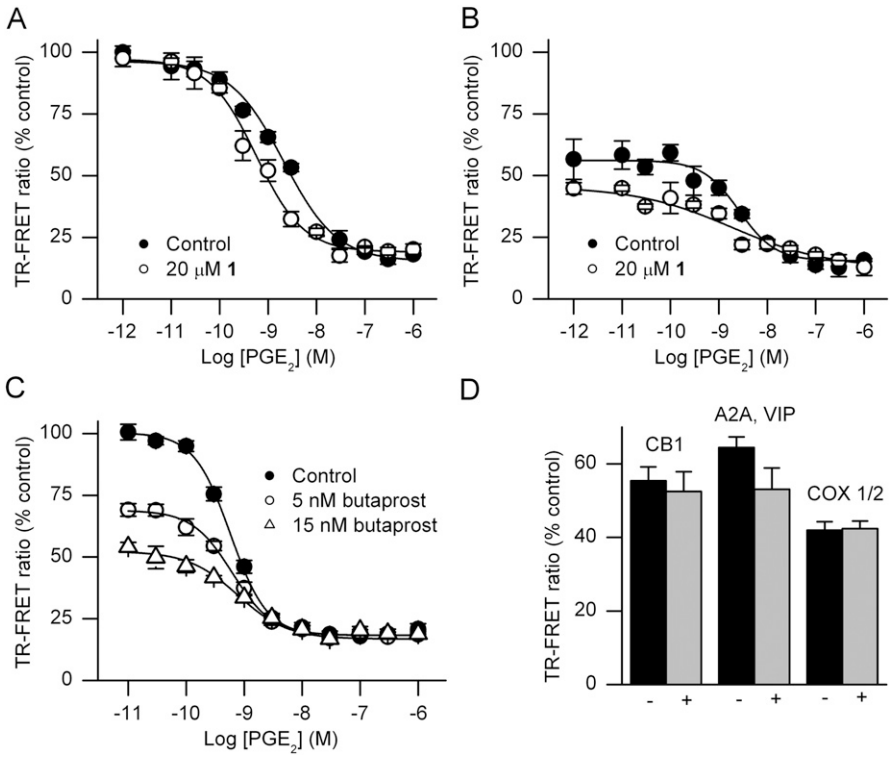

Fig. S7. Behavior of EP2 allosteric potentiators when cAMP is elevated. (*A*) In HCT-15-EP2 cells, elevation of basal cAMP level by preactivation of EP2 with 1 nM PGE_2 changes the profile of compound **1**. In the absence of added PGE_2, 20-μM **1** produces no "basal effect" and increases the potency of PGE_2 from 2.10 nM to 0.57 nM; the slope factor of the logistic fit was 0.79 in control and 0.89 in compound **1**. (*B*) After preincubation with 1-nM PGE_2, compound **1** produces an apparent basal effect, causes a smaller apparent increase in the potency of PGE_2 (from 2.60 nM to 1.86 nM), and the logistic fit displays a shallow slope (1.16 in control vs. 0.43 in compound **1**). (*C*) The potency of PGE_2 as an EP2 agonist is not increased in the presence of the EP2 agonist, butaprost. The EC_{50} of PGE_2 was 0.58 nM in control, 0.63 nM after preincubation with 5 nM butaprost and 0.78 nM in 15 nM butaprost. (*D*) The elevation of cAMP (reduced TR-FRET ratio) caused by 20 μM **1** in C6G-EP2 cells in the absence of added PGE_2 was not prevented by preincubation with a CB1 receptor blocker, a mixture of antagonists of adenosine and VIP receptors, or a mixture of COX1/2 inhibitors. Shown are the mean ± SEM of quadruplicate measurements in a single experiment; the experiment was repeated at least three times with similar results.

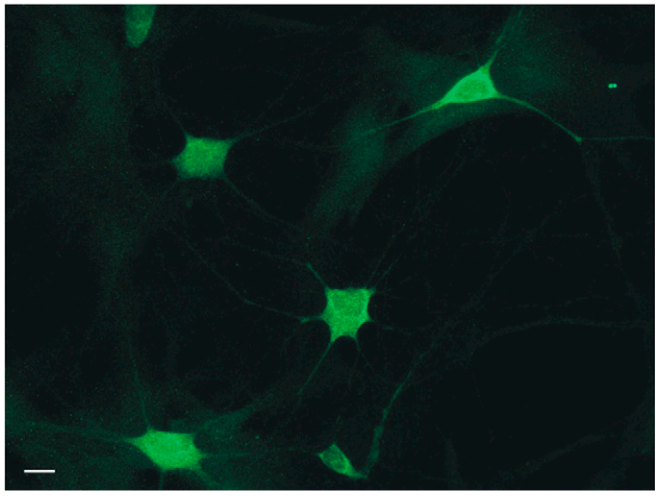

Fig. S8. EP2 expression in hippocampal culture. EP2 receptor (*green*) expression is widespread in hippocampal cultures (DIV 14). (Scale bar, 10 μm.)

Table S1. Predicted adsorption, distribution, metabolism, and excretion properties of the EP2 allosteric compounds by QikProp

	QPlogPo/w[a]	QPlogS[b]	QPPCaco[c]	QPPMDCK[d]	QPlogBB[e]
	Range or recommended values[f]				
Compound	-2.0 - 6.5	-6.5 - 0.5	< 25 poor > 500 great	< 25 poor > 500 great	-3.0 - 1.2
1	3.901	-5.036	1,460	1,250	-0.427
2	4.68	-5.926	1,960	1,480	-0.345
3	3.306	-4.441	1,440	1,100	-0.385
4	4.966	-6.287	2,000	2,770	-0.223
5	3.336	-4.312	143	114	-0.744
6	4.003	-4.468	1,850	1,390	-0.357
7	5.19	-6.382	2,540	1,990	-0.222
8	3.662	-3.94	147	119	-0.712
9	4.623	-5.769	1,930	1,480	-0.336
10	3.568	-4.692	898	606	-0.566
11	3.308	-4.438	887	631	-0.566
12	3.624	-4.794	990	1,078	-0.444
13	4.034	-5.246	1,739	1,344	-0.318
Doxorubicin	-0.514	-2.925	1.33	0.425	-3.461

[a]Predicted octanol/water partition coefficient.
[b]Predicted aqueous solubility, log S. S in mol/L is the concentration of the solute in a saturated solution that is in equilibrium with the crystalline solid.
[c]Predicted apparent Caco-2 cell permeability in nm/s. Caco-2 cells are a model for the gut–blood barrier.
[d]Predicted apparent MDCK cell permeability in nm/s. MDCK cells are a good mimic for the blood–brain barrier.
[e]Predicted brain–blood partition coefficient.
[f]Range is for 95% of known drugs.